PNC TN941 81－42

Activities in the SBL-FPL Loops for LMFBR Safety Studies(II)

April, 1981

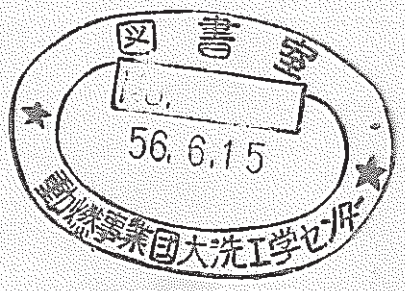

POWER REACTOR AND NUCLEAR FUEL
DEVELOPMENT CORPORATION

複製又はこの資料の入手については、下記にお問い合わせ下さい。

〒311-13　茨城県東茨城郡大洗町成田町4002

動力炉・核燃料開発事業団　大洗工学センター

システム開発推進部　技術管理室

Inquiries about copyright and reproduction should be abbressed to: Technology Management Section, O-arai Engneering Center, Power Reactor and Nuclear Fuel Development Corporation 4002, Narita O-arai-machi Higashi-Ibaraki-gun, Ibaraki, 311-14, Japan

動力炉・核燃料開発事業団 (Power Reactor and Nuclear Fuel Development Corporation)

PNC TN941 81－42
April, 1981

Activities in the SBL-FPL Loops for LMFBR Safety Studies (II)

Edited by Kazuo HAGA*

CONTENTS

This report is a revised version of "Activities in SBL-FPL Loops for Safety Study of LMFBR(I)" PNC N941 79-19 (June 1979).

Fast Reactor Safety Section, Steam Generator Division,
O-arai Engineering Center,
Power Reactor and Nuclear Fuel Development Corporation
O-arai, Ibaraki-ken, 311-13 Japan
Telephone: 02926-7-4141

* Fast Reactor Safety Section, Steam Generator Division,
O-arai Engineering Center, PNC.

List of Figures

A. Introduction

As the first step for the safety study of liquid metal cooled fast breeder reactors (LMFBR's), it is necessary to understand the initial events of potential accidents in an LMFBR. Local faults and sodium boiling can be considered in that area. SBL* and FPL** were constructed to investigate such phenomena experimentally. The two loops share one sodium dump tank and the purification system. SIENA (Sodium Installation for Experiment of Nuclear Reactor Safety Analysis) is the generic name given to both loops. A schematic diagram of SIENA is shown in Fig. 1.

The specification of SIENA is as follows.

Main line, Material: stainless steel SUS316 (partly Hastelloy-X)
Inner diameter: 53.3 mm (2B sch 20S)
Design temperature: 600°C (partly 750°C --- lines from test sections to the expansion tank or the head tank)

Power supply system to test section	Total	650kW
	No. 1 System	150kW
	No. 2 System	500kW
Pump head	2 kg/cm^2 at 300 liters/min	
Number of test section	3	
Sodium inventry	1350 kg	

In almost all experiments, electrically heated fuel pin simulators are used in a pin bundle geometry. Figure 2 shows a 37-pin bundle which was installed in the T-3 test section.

The experimental studies using SBL-FPL are conducted by the Core Safety Sodium Behavior Experiment Group (CSSBEG) which belongs to Fast Reactor Safety Section, O-arai Engineering Center, PNC.

Besides SIENA, CSSBEG operates two water test rigs for the purpose of experiments on large bubble behavior during hypothetical core disruptive accident (HCDA) phase. The same type of sodium experiment is conducted in a test vessel of FPL.

---

* SBL : Sodium Boiling Test Loop
** FPL : Fuel Failure Propagation Test Loop

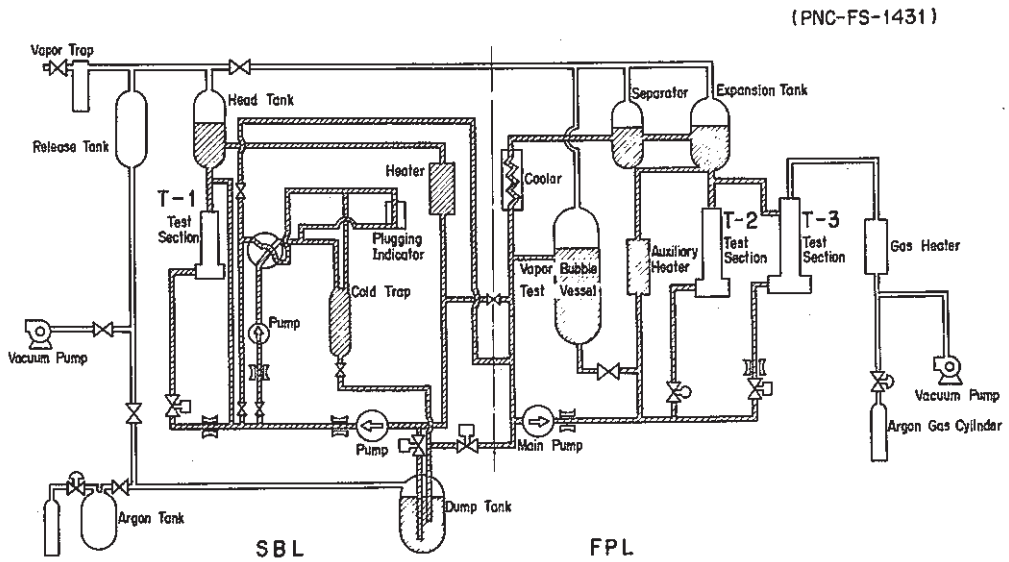

Fig. 1 Schematic Diagram of Sodium Boiling and Fuel Failure Propagation Test Loops

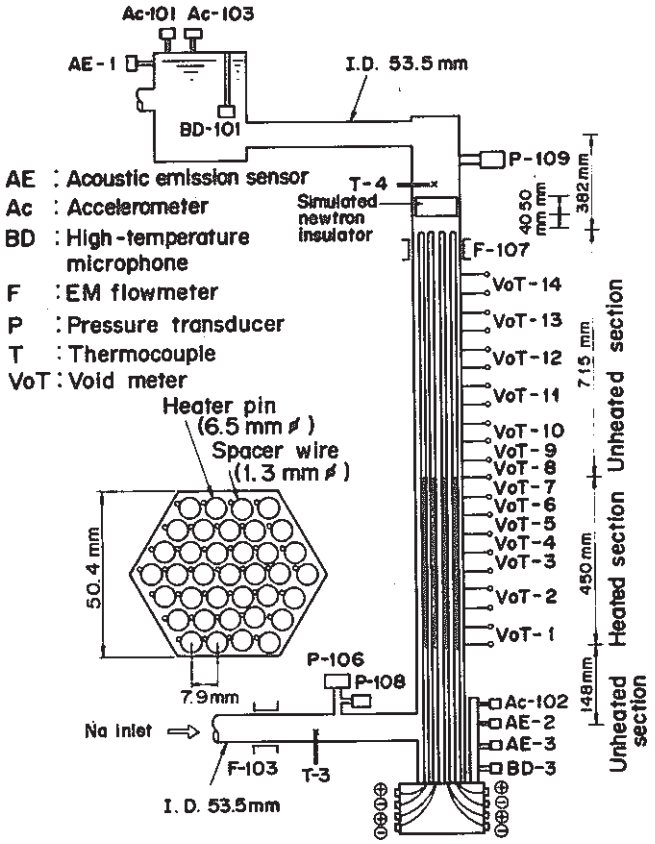

Fig. 2 37F test section
[Ref. C-7] (PNC-FS-962)

B. Fuel Failure Propagation

A local initiating event, such as pin contact, local flow blockage or cladding failure, may successively cause the failure of adjacent fuel pins by the local deterioration of cooling capability. These studies were not only to understand the failure propagation phenomena, but also to investigate the possibility of anomaly detection.

B.1 Fuel Pin Contact

1. Objectives

(1) Investigate experimentally pin surface temperature rise under fuel pin contact conditions.

(2) Develop a computer code to predict temperature distribution under fuel pin contact conditions.

2. Schedule (calender year)

| 1970 - 75 | 76 | 77 | 78 | 79 | 80 | 81 | 82 |

Experiments

e.1, e.2, e.3, e.4

Analyses

a.1 a.2

Experiments:

e.1: 2-pin point contact experiment

e.2: 2-pin line contact experiment

e.3: 3-pin contact experiment

e.4: 7-pin contact experiment

Analyses:

a.1: PICO-I code development

a.2: PICO-II code development

3. Summary

a. Experiments (e.1 -e.4)

Figure 3 is an example of test results and shows an axial pin surface temperature profile under 3-pin contact condition. Figure 4 shows the effect of the flow velocity on the temperature rise in the same pin bundle.

The all test bundles geometries and the temperature rise estimated by the PICO-I code are summarized in Fig. 5.

b. Analyses (a.1-a.2)

(1) PICO-1 is based on the HECTIC-II code and considers a special subchannel between a bowed pin and a normal pin.

(2) PICO-II is a revised version of PICO-I. The main improved points from the original are as follows:

a. The flow redistribution was considered. As the base of the hydrolic model, PICO-II adopted that of the COBRA-II code.

b. A routine to calculate the inner temperature profile of a pin was added.

4. Future works

Analysis of experimental data by PICO-II code.

5. References

[B.1-1] K. Haga et al., "The effects of Bowing Distortions on Heat Transfer in a Seven Pin Bundle," ASME paper, 74-WA/HT-50 (1974)

[B.1-2] M. Uotani et al., "The Effect of Fuel Pin Contact on Local temperature Rise in LMFBR Fuel Subassembly," Proceedings of International Meeting on Fast Reaction Safety Technology p.2553-p.2561, Seattle (1979)

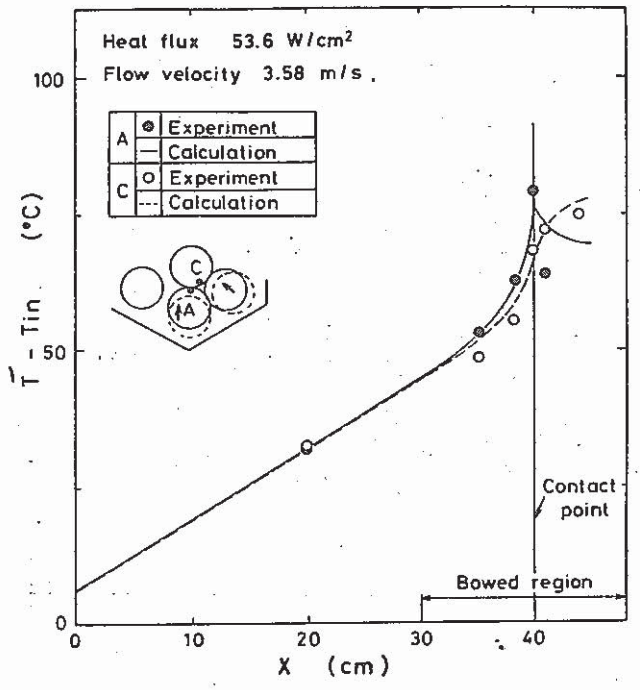

Fig. 3 Axial temperature distribution of bowed pin in case of three-pin contact [Ref. B.1-2, Fig. 8]

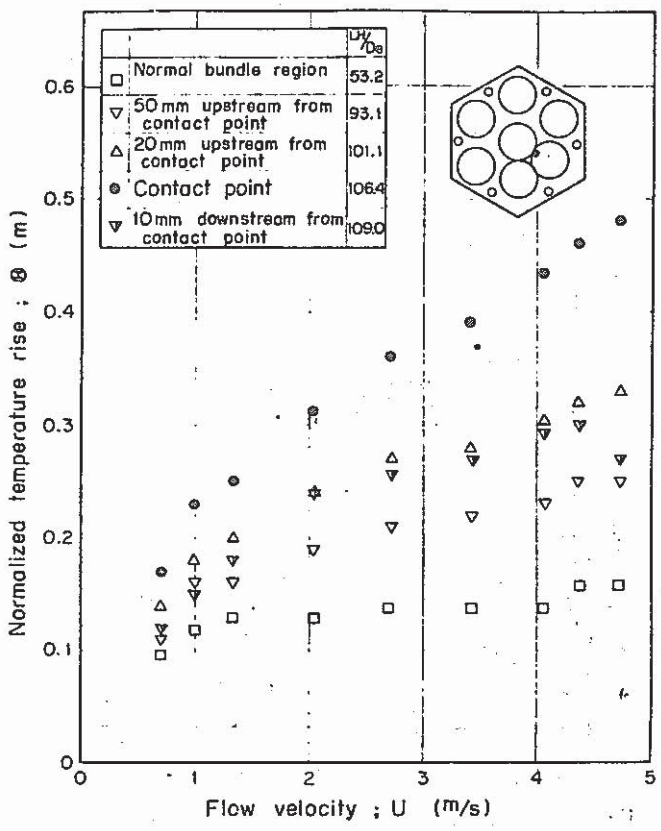

Fig. 4 Normalized temperature rise of bowed pin in case of three-pin contact [Ref. B.1-2, Fig. 7]

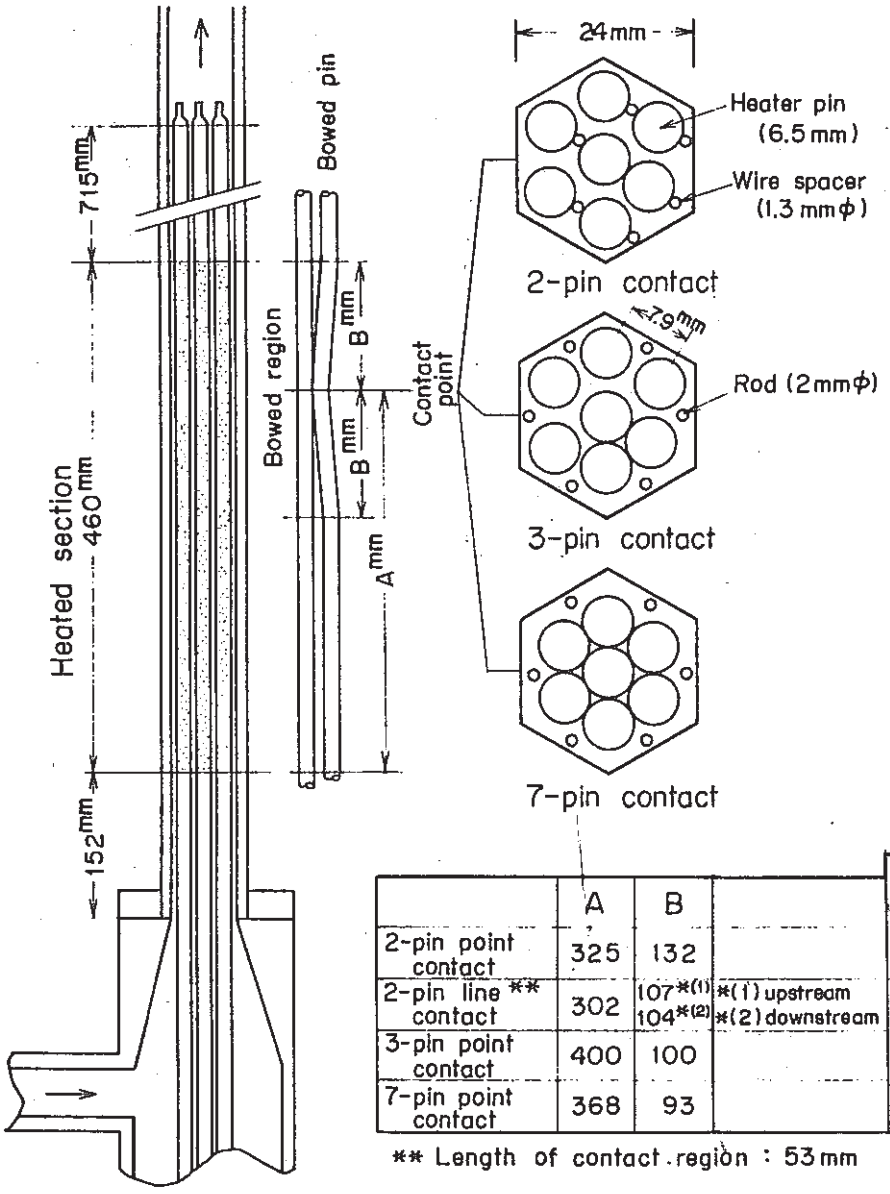

	A	B		Temperature rise at MONJU conditions
2-pin point contact	325	132		40 degree C
2-pin line ** contact	302	107*(1) 104*(2)	*(1) upstream *(2) downstream	70
3-pin point contact	400	100		100
7-pin point contact	368	93		150

** Length of contact region : 53 mm

Fig. 5 Fuel pin contact test bundles [Ref. B.1-2, Fig. 5]

B.2 FP Gas Release

1. Objectives

(1) Investigate thermal and mechanical effects caused by fission product gas release into a heated pin bundle.

(2) Reveal the effect of entrained gas on heat transfer.

2. Schedule

| 1974 - 75 | 76 | 77 | 78 | 79 | 80 | 81 |

Experiments

e.1: Normal 37-pin bundle experiment

e.2: Sodium-gas two phase flow experiment in annular flow channel (single-pin)

e.3: Locally blocked 37-pin and 61-pin experiments (Refer to Section B.3)

e.4: Locally blocked 91-pin experiment (Refer to Section B.3)

3. Summary

e.1: (1) Transient and continuous injection of argon gas into a 37-pin bundle test section from a gas injector pin (Fig. B.2-1).

(2) The largest temperature increase was observed on the gas impingement target pin surface. The heat transfer coefficient at the gas impingement surface was lowered below 1/4 of those at initial (single-phase liquid) conditions. The temperature history of that surface compared well with SURFACE code calculations using experimentally obtained heat transfer coefficients. (Fig. 6, Fig. 7)

(3) Measured sodium pressure pulse during gas injection was below 1/5 of initial gas plenum pressures. Neither damage nor deformation was observed in the pin bundle after the experiments.

e.2: (1) Sodium-gas two-phase flow heat transfer experiments were conducted with a single-pin, annular flow channel test section.

(2) Decrease in heat transfer coefficient was less than that in the gas impingement experiments (e.1).

e.3: (1) Argon gas was injected into a partially blocked 37-pin bundle.

(2) The temperature in the wake region indicated a conspicuous increase when the sodium velocity was higher than 2 m/s due to

the gas concentration in the region. However in lower velocity conditions, less than 2 m/s, the temperature rise was little.

(3) The highest temperature rise was observed downstream of the gas injection section.

(4) For an increasing gas release rate, the temperature rise increased in the range up to 0.6 g/s of gas.

4. Future work

Gas release behind blockage in a 91-pin bundle under non-boiling and boiling conditions will be studied.

5. References

[B.2-1] K. Haga et al., "Fission Gas Release Experiment in a Simulated LMFBR Subassembly," Trans. ANS Vol. 34 p.494-p.495 (1980)

[B.2-2] H. Kondoh et al., "Sodium-gas Two-phase Flow Heat Transfer in Eccentric Annuli," 15th Japan Heat Transfer Symposium (1978) (Japanese)

[B.2-3] F. Namekawa et al., "Gas Release Experiment in a Locally-Blocked Simulated Fuel Subassembly," Proceedings of Atomic Energy Society of Japan Fall Meeting B 79 (1979) (Japanese)

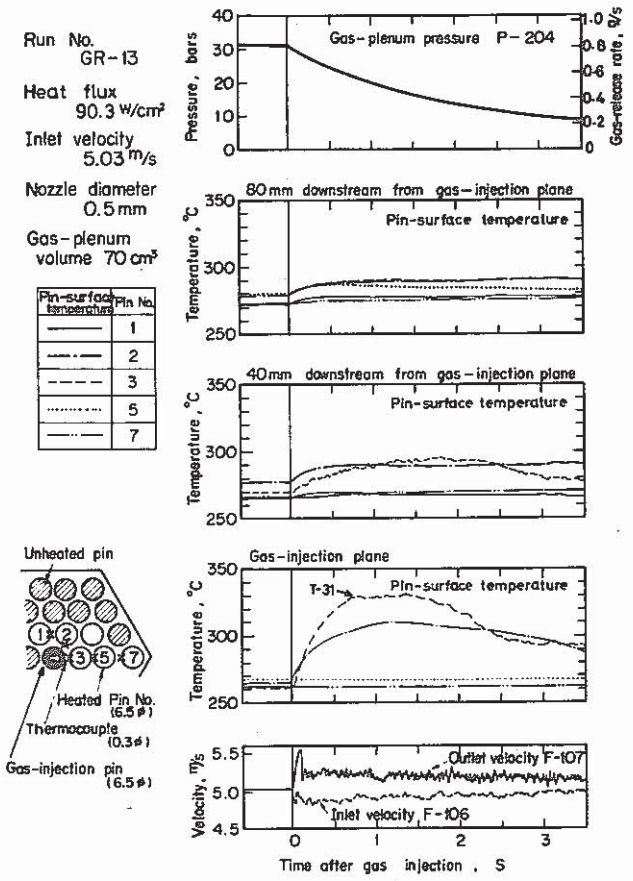

Fig. 6 Signals from flowmeters, thermocouples and pressure transducer for a transient gas-release test [Ref. B.2-2] (PNC-FS-334)

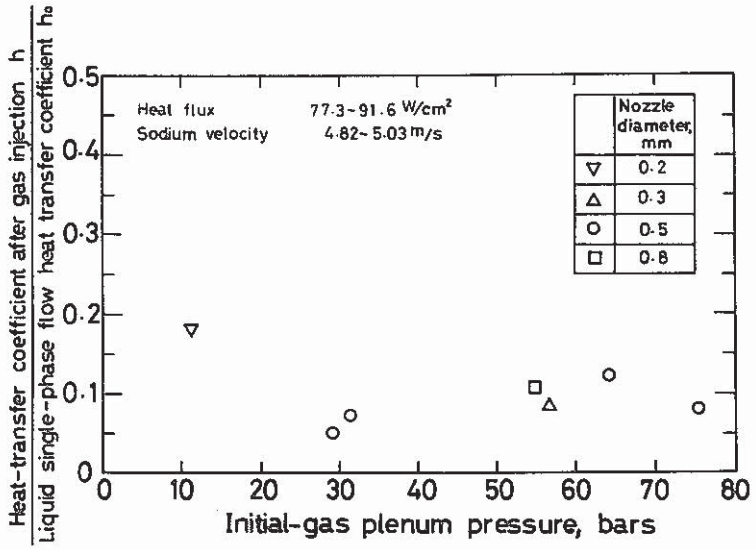

Fig. 7 Ratio of heat-transfer coefficient after gas-injection to liquid single-phase flow heat-transfer coefficient in impingement area for transient gas-release tests [Ref. B.2-1] (PNC-FS-335)

B.3 Local Blockage

1. Objective

(1) Investigate the temperature rise caused by a local flow blockage with and without accompanying FP gas release behind the blockage.

(2) Evaluate dryout criteria due to local boiling.

2. Schedule

| 1970 - 75 | 76 | 77 | 78 | 79 | 80 | 81 | 82 |

Experiments

Analyses

Experiments (single-phase):

e.s.1: 7-, 19- and 37-pin bundle experiments

e.s.2: 61-pin bundle experiment

e.s.3: 91-pin bundle experiment

Experiments (local boiling):

e.b.1: 7-, and 37-pin bundle experiments

e.b.2: 61-pin bundle experiment

e.b.3: 91-pin bundle experiment

Analyses (local boiling):

a.1: SPHERE code

a.2: BOCAL code

3. Summary

Experimental results:

e.s.1 ~ e.s.3: The temperature distributions behind blockages were measured. (Fig. 8)

Figure 9 shows calculated temperature rises in the wake region in the central blockage and edge blockage cases, which were obtained from the residence time of the coolant.

Based on the residence time concept an universal correlations were obtained to evaluate local temperature rise. In Fig. 10 calculated dimensionless residence times from experiments are plotted against a new dimensionless variable named, Ring Parameter (= characteristic length of

blockage, D_B, divided by pin pitch, P). Almost all data available converged into one line, which is expressed by the empirical formula,

$$\tau U_B/d_h = \frac{C_p}{4} \quad \frac{U_o}{q\ (1-F)} \quad (T_{wk}-T_c) = 35.3(D_B/P)^{0.85} \quad \cdots\cdots\cdots \quad (1)$$

where

C_p : Specific heat of sodium
d_h : Equivalent diameter of subchannel
F : Fraction of blocked flow area
q : Heat flux
T_c : Average temperature of sodium in main flow
T_{wk}: Average temperature in the wake
U_B : Flow velocity at blocked section
U_o : Inlet flow velocity
τ : Coolant residence time
γ : Specific gravity of sodium

The power 0.85 on the Ring Parameter can be regarded as the blockage size dependency of the ratio.

Extrapolation to Reactor Conditions

The peaking factors, $C_{B,max}=(T_{B,max}-T_c)/(T_{wk}-T_c)$ and $C_w=(T_w-T_c)/(T_B-T_c)$, were obtained, where T_B means an apparent local tremperature in the wake that will be observed in case of bare bundle and T_w is the real local temperature under wire-wrapped bundle configuration. From many temperature data measured rotationally at different positions on the same axial location it was estimated that the peaking factor C_w varies from 0.9 to 1.2. The bare bundle factor, $C_{B,max}$, was 1.5 to 1.6.

These values were directly multiplied by the wake temperature estimated from Eq.(1). The resultant local temperature increase for the reactor conditions are shown in Fig. 11.

e.b.1 ~ e.b.2: Stable oscillatory boiling was observed in a wide range of conditions (Fig. 12, Fig. 13). In the tests, the heat flux was increased stepwise with the other conditions being held almost constant. Figure 14 shows the signals observed during the occurrence of permanent dryout.

The theoretical excess temperature at the instant of dryout, which was equal to the temperature exceeding saturation temperature and was

calculated from a simple heat balance equation, was nearly 140°C. The excess temperature was correlated to the subcooled temperature measured at the axial end of the wake region at the instant of boiling inception. Many available data were also reviewed. The margin to the boiling crisis was found to depend on the subcooled temperature, i.e. a decreasing function of power to flow ratio, q/U_o. It was thus concluded that there may be a sufficiently large margin for the actual fuel subassembly in an LMFBR to avoid dryout.

a.1: SPHERE is a one-dimensional boiling code which calculates the oscillation of a sperical bubble.

a.2: BOCAL is a two-dimensional boiling code which is under development.

4. Future works

Conduct experiments in a 91-pin bundle with edge blockage.

Make clear the dryout conditions of local boiling.

5. References

[B.3-1] M. Uotani et al., "Local Flow Blockage Experiment in 37-pin Sodium Cooled Bundle with Grid Spacers" 8th Liquid Metal Boiling Working Group Meeting, Mol (1978)

[B.3-2] K. Yamaguchi et al., "Local Temperature Rise and Boiling Behavior behind a Central Blockage in a Wire-Wrapped Pin Bundle," 9th Liquid Metal Boiling Working Group Meeting, Casaccia (1980)

[B.3-3] M. Uotani et al., "Sodium Boiling Experiment in a Pin Bundle Geometry," Proceedings of Atomic Energy Society of Japan Annual Meeting A24 (1980) (Japanese)

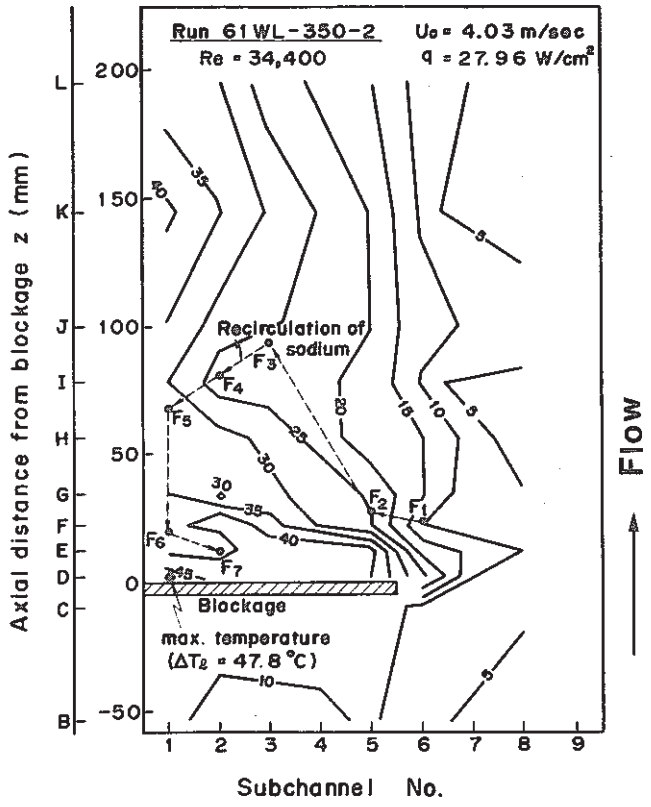

Fig. 8 Isotherms($T-T_{in}$) of sodium behind the blockage [Ref. B.3-2] (PNC-FS-1086)

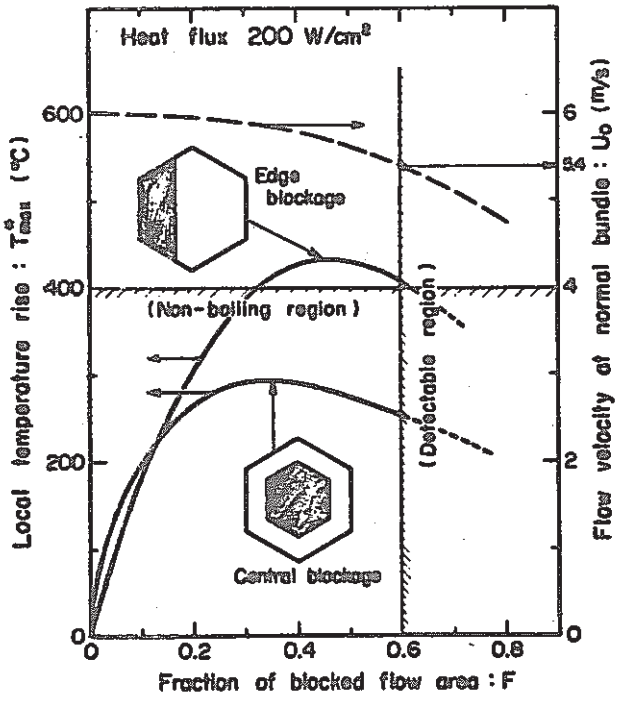

Fig. 9 Relation between local temperature rise($T-T_{in}$) in the wake region and fraction of blocked flow area [Ref. B.3-1] (PNC-FS-822)

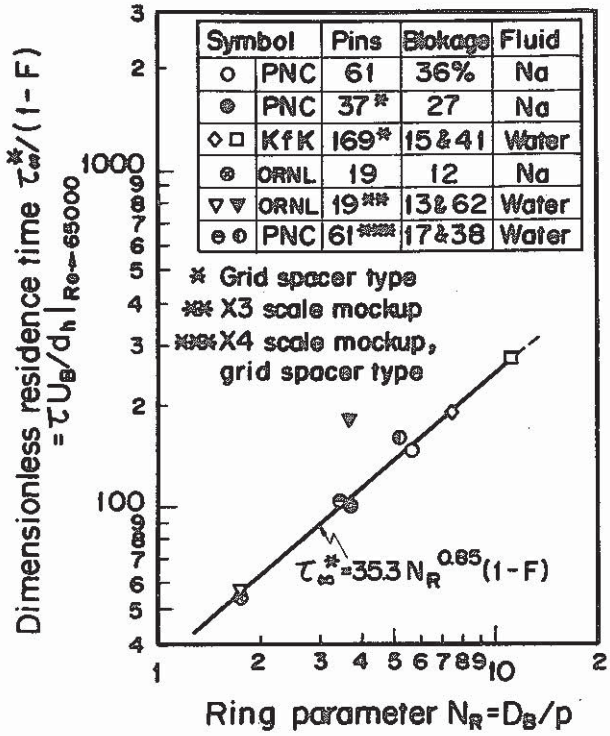

Fig. 10 Correlation between dimensionless residence time and Ring Parameter [Ref. B.3-2] (PNC-FS-1103)

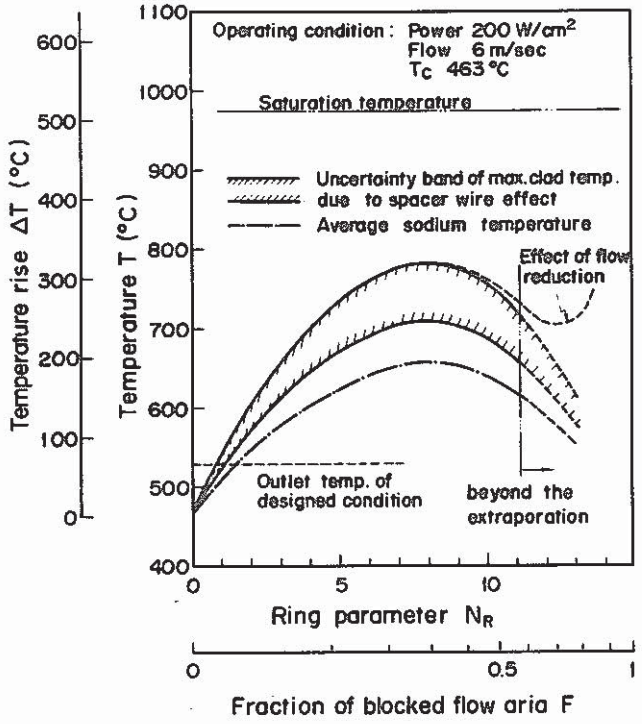

Fig. 11 Estimations of temperature rise behind various blockages, -- MONJU conditions [Ref. B.3-2] (PNC-FS-1107)

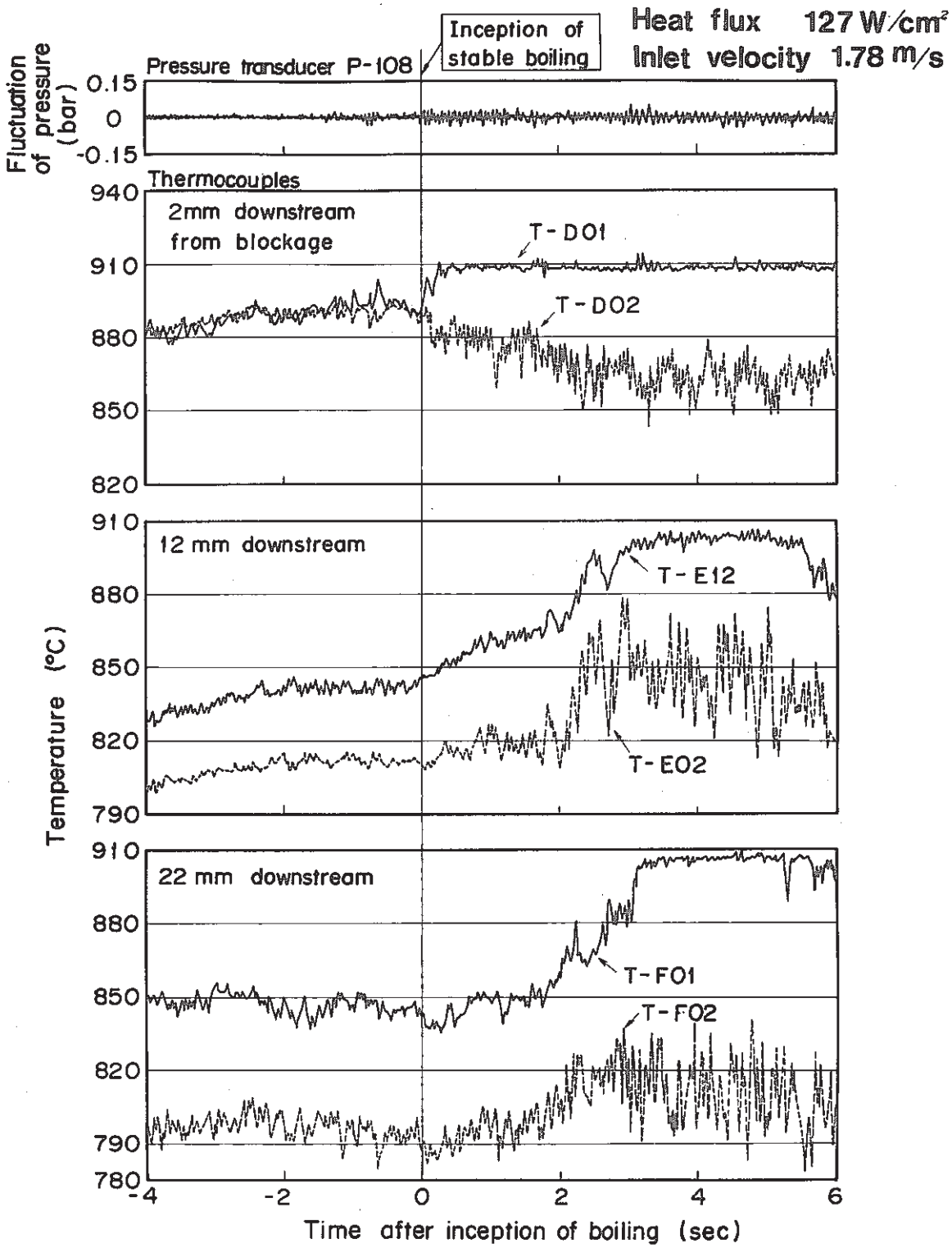

Fig. 12 Pressure and temperature at local boiling inception [Ref. B.3-3] (PNC-FS-1006)

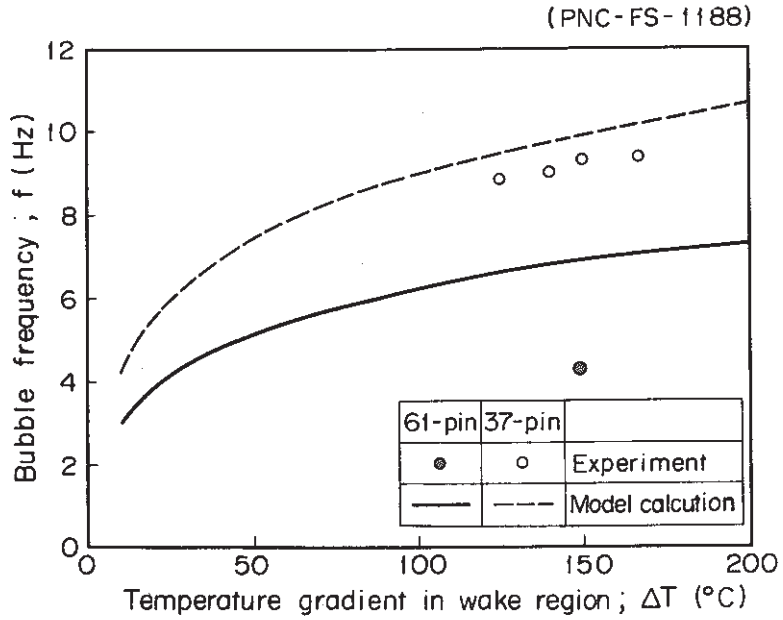

Fig. 13 Effect of temperature gradient in the wake region on the oscillation frequency [Ref. B.3-3] (PNC-FS-1188)

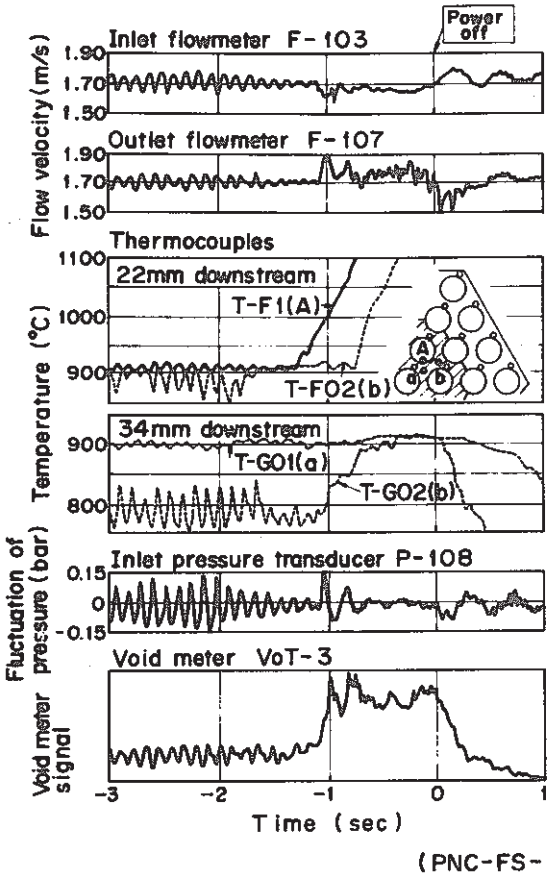

Fig. 14 Signals at the occurrence of permanent dryout, -- Run No. 37 (19) WLB-114 [Ref. B.3-2] (PNC-FS-1109)

B.4 Anomaly Detection

1. Objective

Estimate the possibility of anomaly detection in a reactor system by using outlet temperature and flow fluctuations or acoustic sensors.

2. Schedule

| 1976 | 77 | 78 | 79 | 80 | 81 |

Experiments in pin bundle geometries and analysis
(refer Sections B.2 and B.3)

3. Summary

a. Outlet temperature and flow fluctuations

(1) The temperature fluctuation caused by local blockage can hardly transfer to the end of a pin bundle unless the temperature field is changed. (Fig. 15, Fig. 16, Fig. 17)

(2) The strong correlation was found for the temperature fluctuations observed at the boiling position and at the end of the bundle, while the correlation has not been clarified with regard to the fluctuations at the subchannel outlet. (Fig. 18)

(3) It appears possible to detect a local boiling accident when the boiling intensity becomes fairly large.

(4) The burst-type one pin failure can be detected by the flow fluctuations. (Fig. 19)

(5) The whiteness test method (WTM) applied to a fluctuation signal was a sensitive and reliable method for detecting a local accident within a subassembly.

b. Boiling acoustic noise measured by accelerometer

The boiling causes a considerable increase in acoustic noise intensity at all frequencies, particularly in the high frequency ranges (5kHz ~ 100 kHz)(Fig. 20). The broad peak observed at approximately 10 kHz is possibly attributed to the sodium vapor collapse phenomenon.

4. Future works

Conduct experiments in a locally blocked 91-pin bundle.

Make clear the detectable range of local boiling by outlet temperature and flow fluctuations.

Measure boiling noise by sodium immersed-type sensors.

5. References

[B.4-1] Y. Kikuchi et al., "Temperature, Flow and Acoustic Noises in a

Locally Blocked 37-Pin Bundle," 7th Liquid Metal Boiling Working Group Meeting, Petten (1977)

[B.4-2] Y. Ozaki et al., "Acoustic Noises with Loss-of-Flow Sodium Boiling Experiment in a 19-Pin Bundle," 8th Liquid Metal Boiling Working Group Meeting, Mol (1978)

[B.4-3] T. Ogino et al., "Feasibility Study of Local Core Anormaly detection by Use of Temperature and Flow Fluctuations at LMFBR Fuel Subassembly Outlet," Proceedings of International Meeting on Fast Reactor Safety Technology p.2630-p.2650, Seattle (1979)

[B.4-4] H. Inujima et al., "Temperature and Flow Fluctuations under Local Boiling in a Simulated Fuel Subassembly," 9th Liquid Metal Boiling Working Group Meeting, Casaccia (1980)

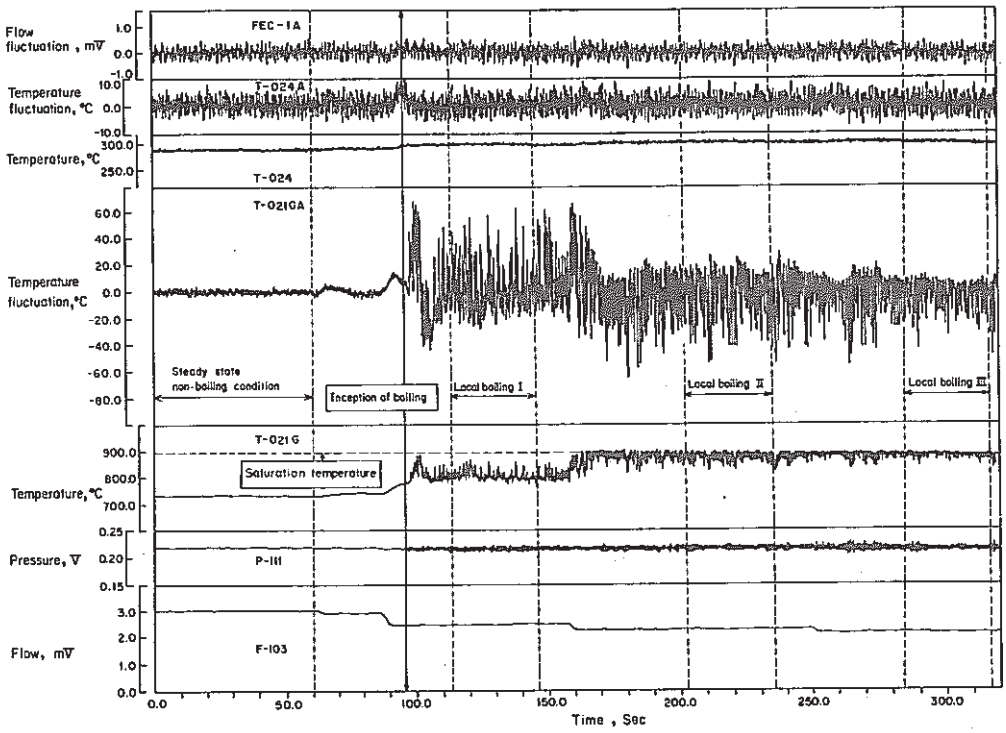

Fig. 15 Signals under local boiling condition (Run No. 61WLB-101) [Ref. B.4-4, Fig. 3]

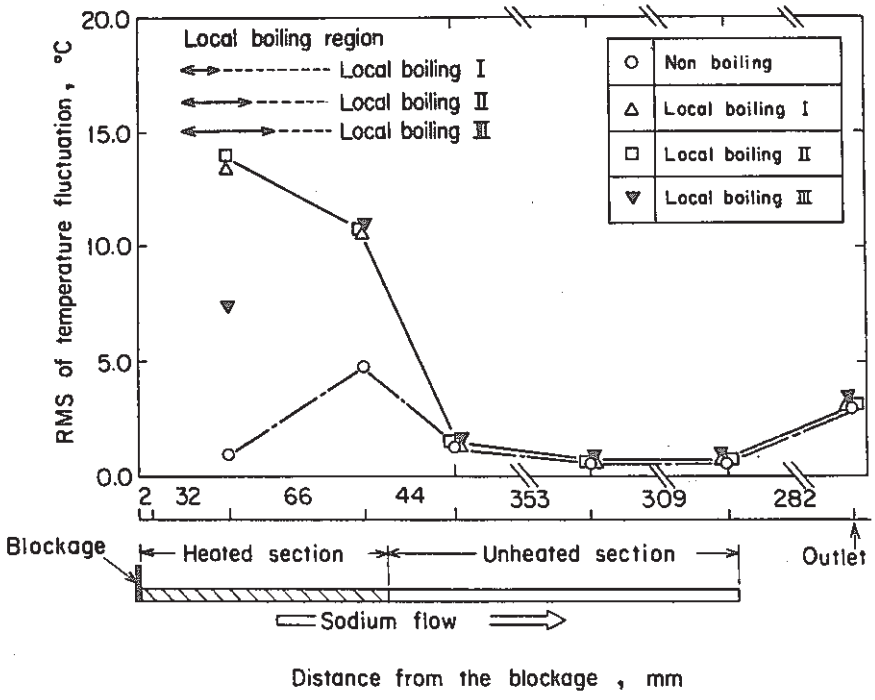

Fig. 16 RMS values of temperature fluctuations observed at several axial positions behind the blockage (Run No. 61WLB-101) [Ref. B.4-4, Fig. 4]

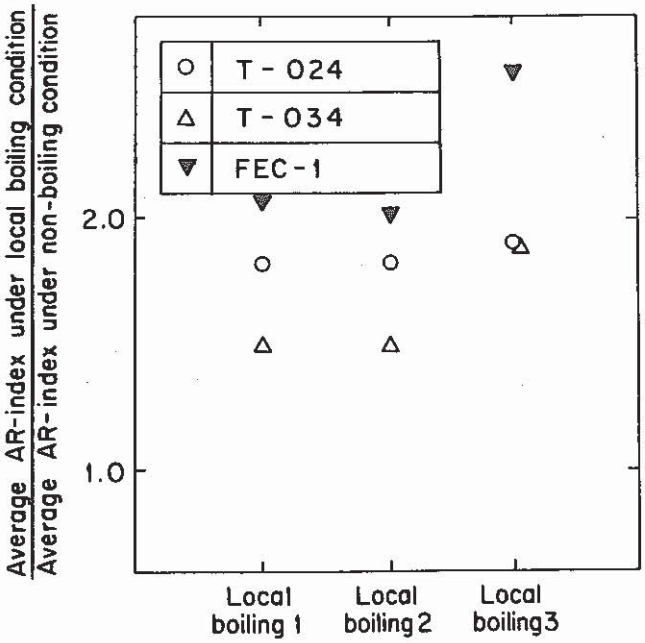

Fig. 17 Ratio of the average AR index under boiling condition to that under non-boiling condition [Ref. B.4-4, Fig. 12] (Run No. 61WLB-101)

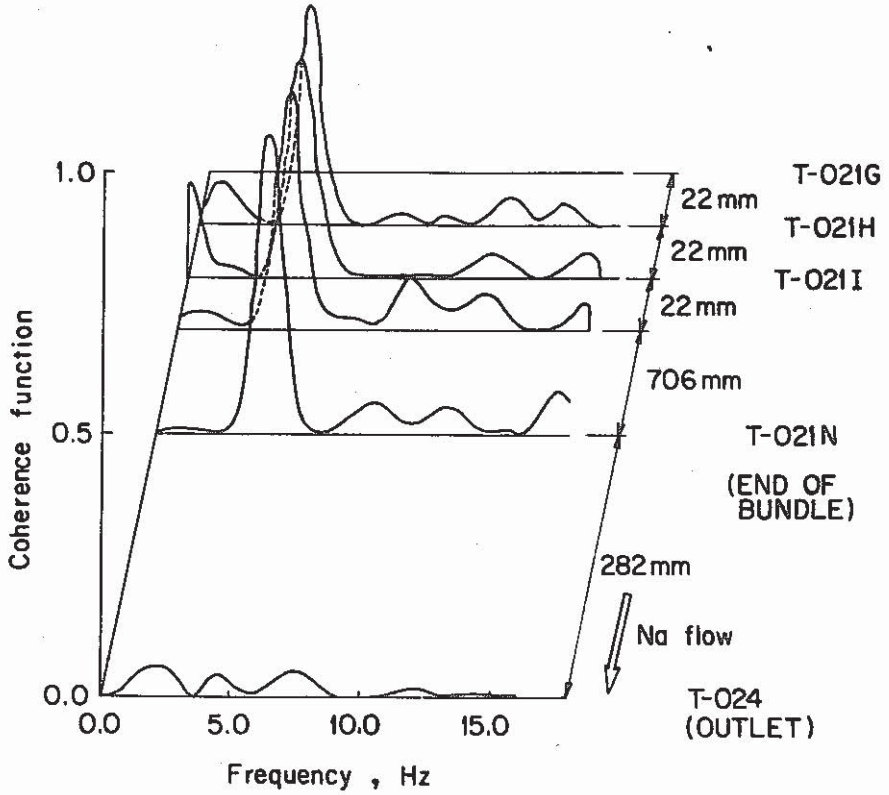

Fig. 18 Coherence functions between several couples of temperature fluctuations, one is T-021G and the opposite is one of the others (T-021H,..., T-024), -- Local boiling III condition [Ref. B.4-4, Fig. 9] (Run No. 61WLB-101)

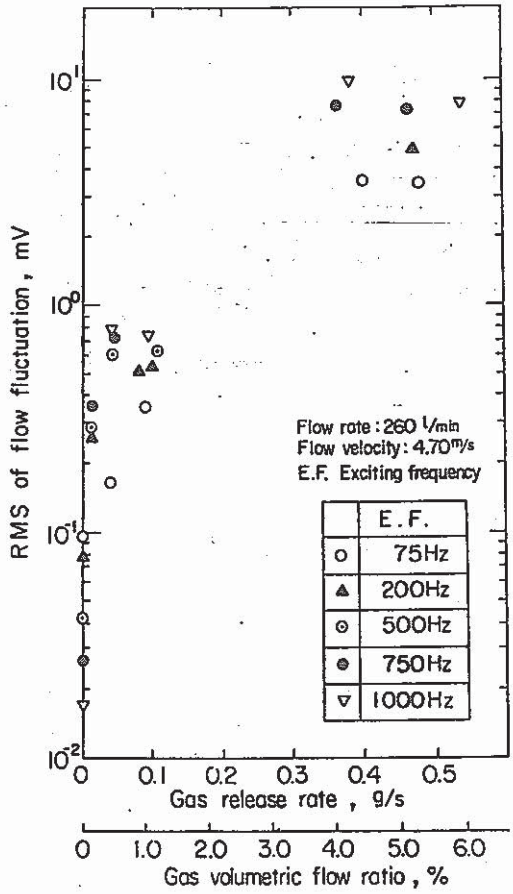

Fig. 19 Effect of gas release rate on RMS value of flow fluctuation [Ref. B.4-3, Fig. 8]

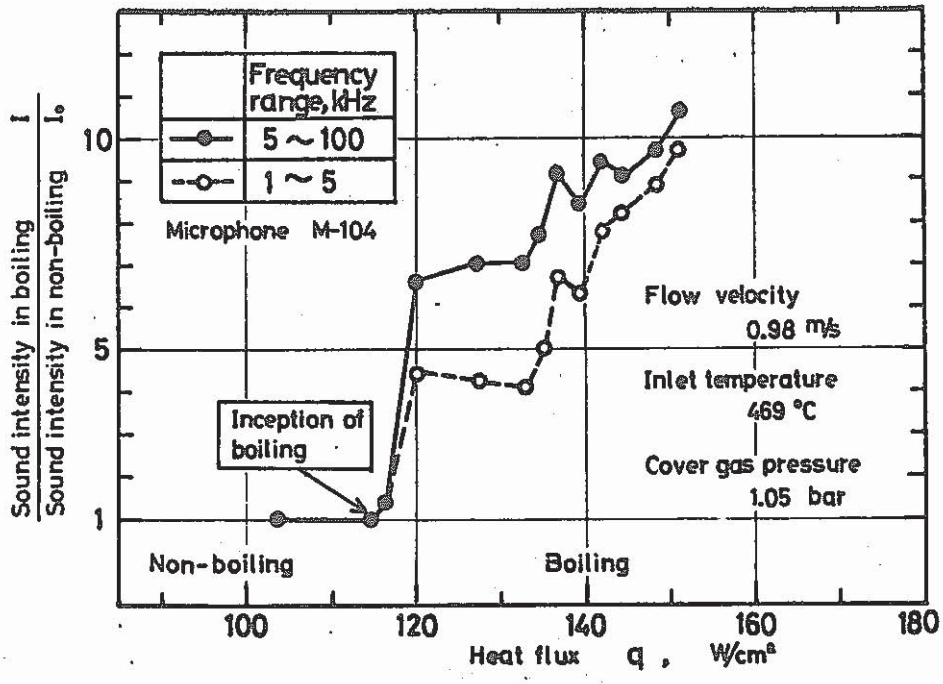

Fig. 20 Effect of heat flux on intensity of acoustic noise with boiling ; run No. 37(12)LB-129 [Ref. B.4-1, Fig. 6]

C. Sodium Boiling

1. Objectives

Understand pin bundle coolability by boiling in low heat flux and low flow rate conditions (which correspond to loss of piping integrity and loss of shutdown heat removal system).

Examine the boiling phenomena at loss of flow condition and transient over power condition.

2. Schedule

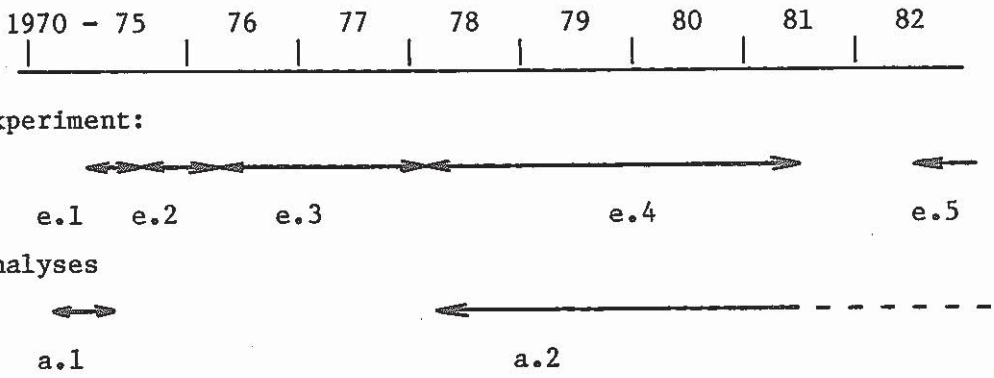

Experiments:

e.1: Single pin experiments

e.2: 7-pin bundle experiments

e.3: 19-pin bundle experiments

e.4: 37-pin bundle experiments (Phase I)

e.5: 37-pin bundle experiments (Phase II)

Analyses:

a.1: NAIS-P2 (single-bubble slug-ejection model)

a.2: BOCAL (2-dimentional boiling analysis code)

3. Summary:

(1) Coolability --- Inception of dryout

A series of 37-pin bundle natural circulation experiments showed the existance of a large "boiling window" under low power condition (Fig. 21). Dryout did not occur in the quality range below 0.5 (Fig. 22).

In LOF-type experiments, dryout took place with flow reversal or with flow decease close to flow reversal.

(2) Superheat

Although some runs showed high superheat of 150° to 185°C, many data were below 50°C. The effects of temperature ramp rate prior to boiling inception, flow rate, system pressure, operating

history and heat flux were unclear. There was a tendency that the superheat takes a smaller value as the pin number of a test section increases.

(3) Residual liquid film thickness

The estimated residual liquid film thickness from the data of single-pin tests is in a range of 0.05 mm - 0.26 mm and tends to decrease as superheat at inception of boiling (IB) increases.

(4) Pressure pulse

The pressure pulses generated during bubble collapse are correlated well with collision of re-entrant liquid columns based on the liquid hammer analysis.

(5) Void pattern

a. LOF-type tests

In the single-pin geometry, the boiling flow regime is characterized as a single bubble expulsion model. On the other hand, in the multi-pin geometry, boiling starts around the central subchannels and gradually extends to outer ones because of the initial presence of sharp temperature profile over the cross section of the test section (Fig. 23). Initial expulsion of liquid slugs at boiling inception is dominated by IB superheat:
The higher the IB superheat is the larger the acceleration of the slugs becomes.
However after a whole cross section was covered by saturated coolant, the void behaves as a one-dimensional slug.

b. TOP-type tests

The boiling pattern under slow TOP conditions was rather a homogeneous flow type. Under rapid TOP conditions, however, the boiling sequence showed a tendency to shift from an early phase of multi-bubble formation to a succeeding phase of large single bubble formation.

c. Steady-state forced convection or natural convection tests

The observed flow regime changed from bubbly flow to slug flow and then to an annular or annular mist flow (Fig. 24).

(6) Sodium single phase flow temperature profile

The radial temperature profiles test bundles were obtained which are suitable for the verification calculations by subchannel mixing codes.

4. Future work

Loss of shutdown heat removal system experiment --- simulated full length of fuel pin and chopped cosine power profile.

5. References

[C-1] Y. Kikuchi et al.,
"Incipient Boiling of Sodium Flowing in a Single-pin Annular Channel,"
J. Nucl. Sci. Technol. Vol. 11, No. 5 (1974)

[C-2] Y. Kikuchi, K. Haga and T. Takahashi,
"Experimental Study of Steady-State Boiling of Sodium Folowing in a Single-pin Annular Channel,"
J. Nucl. Sci. Technol. Vol. 12, No. 2 (1975)

[C-3] Y. Kikuchi et al.,
"Transient Boiling of Sodium in a 19-pin Bundle under Loss-of-Flow Conditions,"
7th Liquid Metal Boiling Working Group Meeting, Petten (1977)

[C-4] Y. Kikuchi et al.,
"Transient Boiling of Sodium in a Single-pin Geometry under Loss-of Flow Conditions,"
J. Nucl. Sci. Technol. Vol. 15, No. 2 (1978)

[C-5] Y. Kikuchi,
"Transient Boiling of Sodium in a Seven-pin Bundle under Loss-of-Flow Conditions,"
J. Nucl. Sci. Technol. Vol. 15, No. 9 (1978)

[C-6] Y. Kikuchi,
"Transient Boiling of Sodium in a Seven-pin Bundle under Transient Overpower Conditions,"
J. Nucl. Sci. Technol. Vol. 16, No. 4 (1979)

[C-7] K. Haga et al., "Decay Heat Removal under Boiling Condition in a Pin-Bundle Geometry,"
9th Liquid Metal Boiling Working Group Meeting, Casaccia (1980)

[C-8] K. Haga et al., "Sodium Boiling Experiment in a Bundle Geometry-13,"
Proceedings of Atomic Energy Society of Japan Annual Meeting C25 (1981) (Japanese)

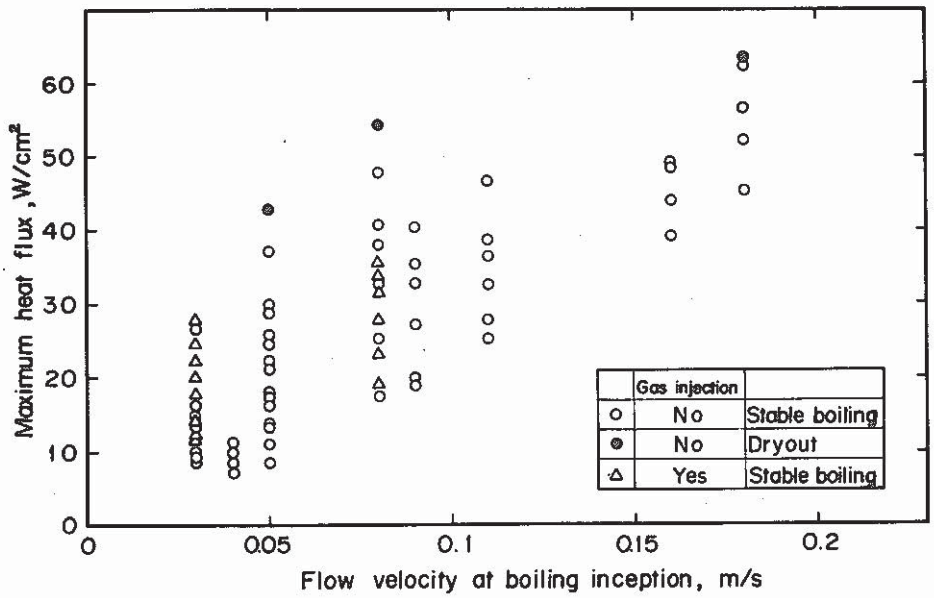

Fig. 21 Experimental conditions of heat fluxes versus initial value of inlet flow velocities [Ref. C-7] (PNC-FS-992)

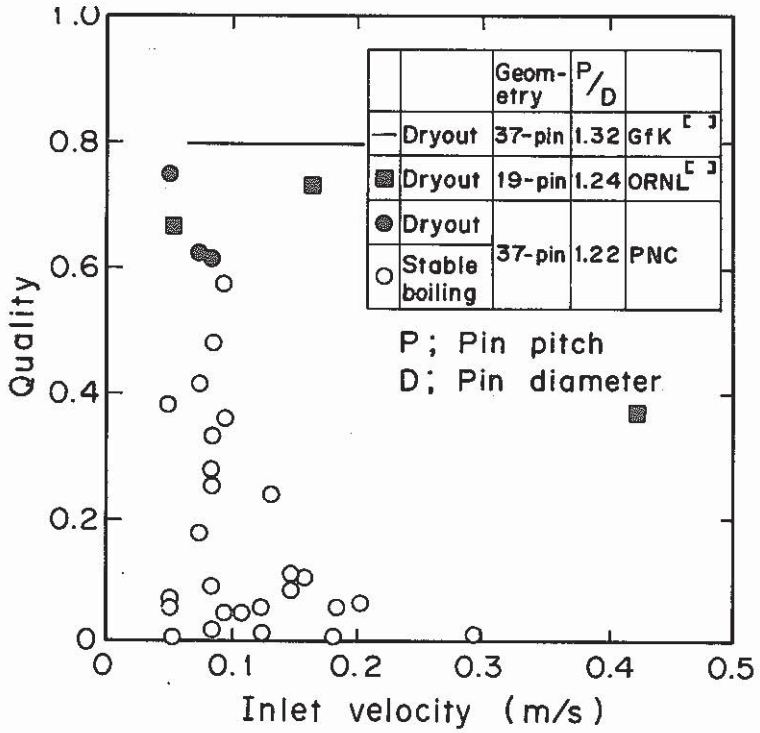

Fig. 22 Comparison between the qualities of the present dryout tests with available data of dryout qualities in pin bundles [Ref. C-7] (PNC-FS-1113)

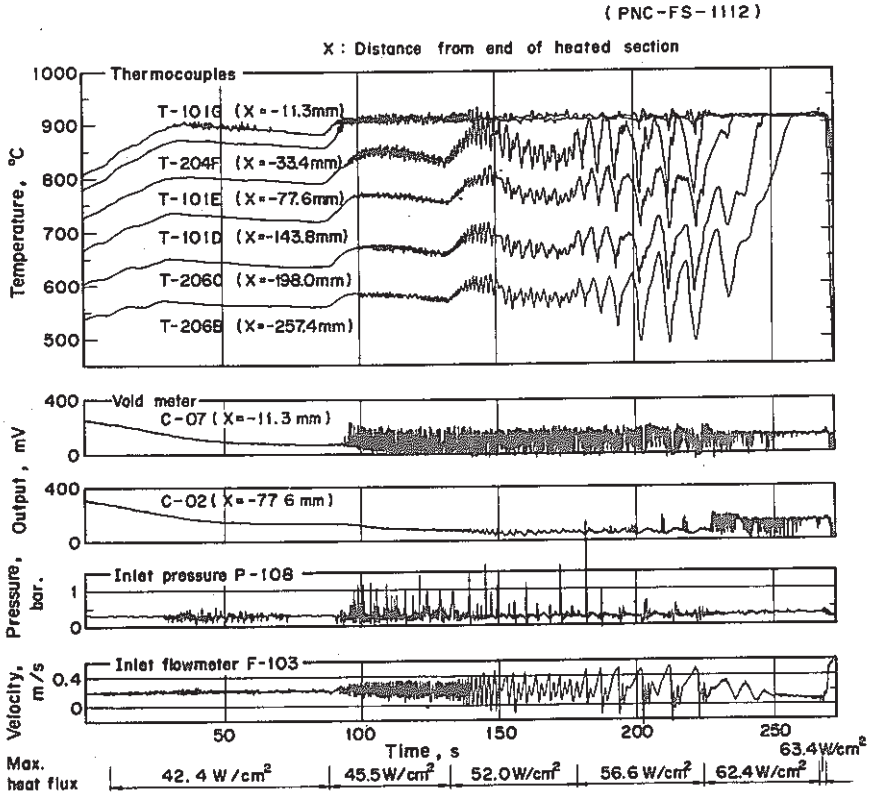

Fig. 23 Signals of sodium temperatures, inlet and outlet flow velocities during the dry-out test, Run No. 37LHF-123 [Ref. C-7] (PNC-FS-1112)

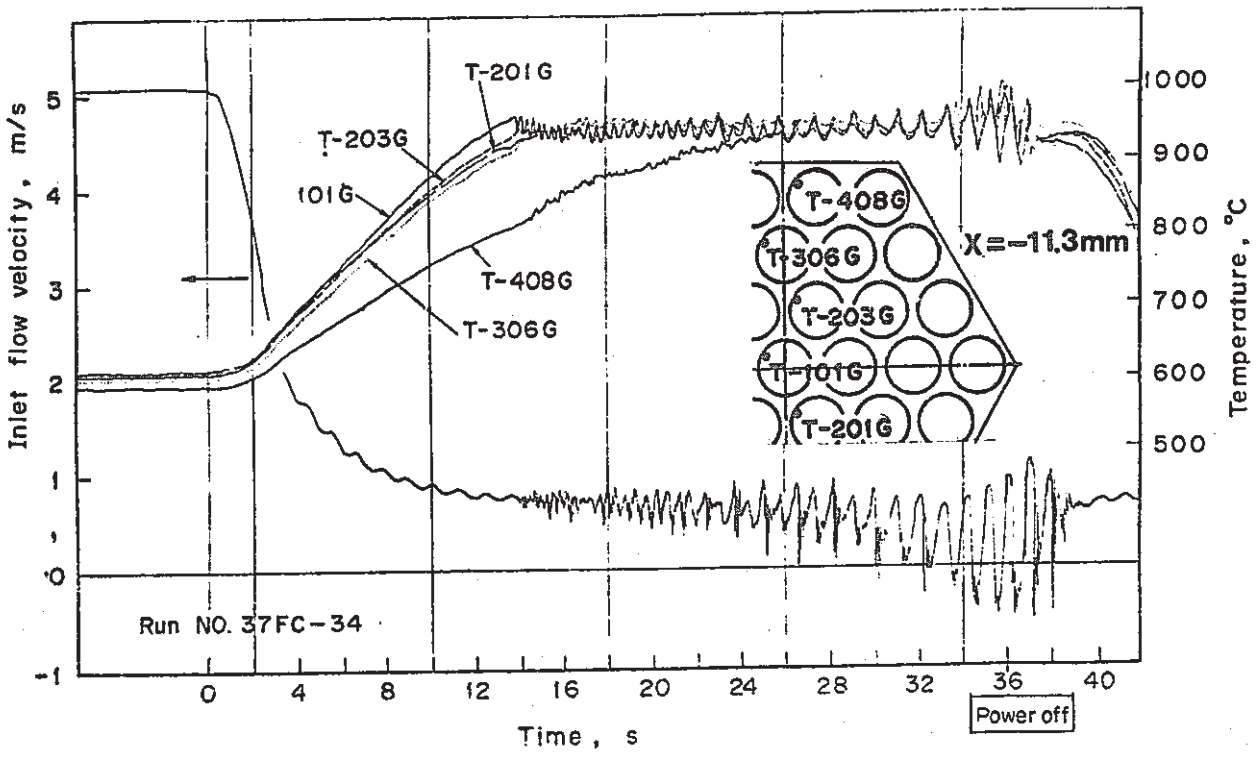

Fig. 24 Signals of inlet velocity and pin surface temeratures during loss-of-flow test, Run No. 37FC-34 [Ref. C-8, Fig. 2]

D. Other Projects

D.1 HCDA Bubble Behavior

1. Objective

Obtain data on HCDA bubble behavior

2. Schedule

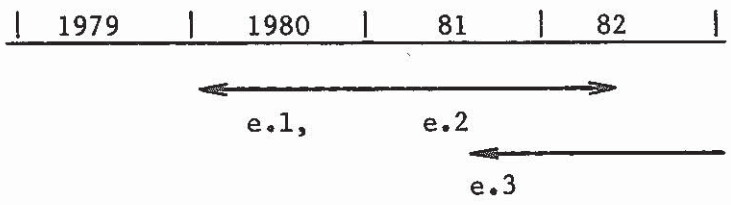

e.1: Buoyant Movement Test

The purposes are to examine the change of bubble shape during the buoyant movement and to determine its driving force. A large water pool (1.2 m x 1.2 m, height of 4 m) named BBT*-I is used for this test (Fig. 25).

e.2: Condensation Test

The condensation of a bubble of vapor and noncondensable gas mixture is optically observed in a hot water pool BBT-II.

e.3: In-Sodium Simulation Test

A vapor bubble test vessel is installed in FPL. It is 800 mm in diameter and around 2000 mm in height. Three vaporizers can be inserted triangularly in the vessel.

D.2 Clad Relocation

1. Objective

Observe melted cladding behavior after dryout of liquid film on fuel pins

2. Schedule

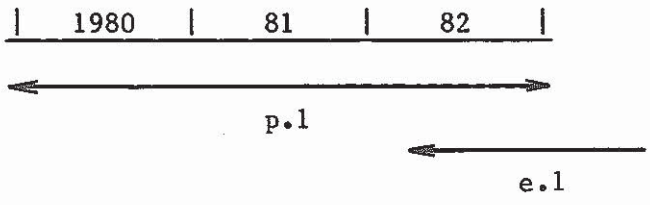

p.1: Development of new-type heater pin for this purpose

e.1: Experiment

---

* BBT: Bubble Behavior Test Rig

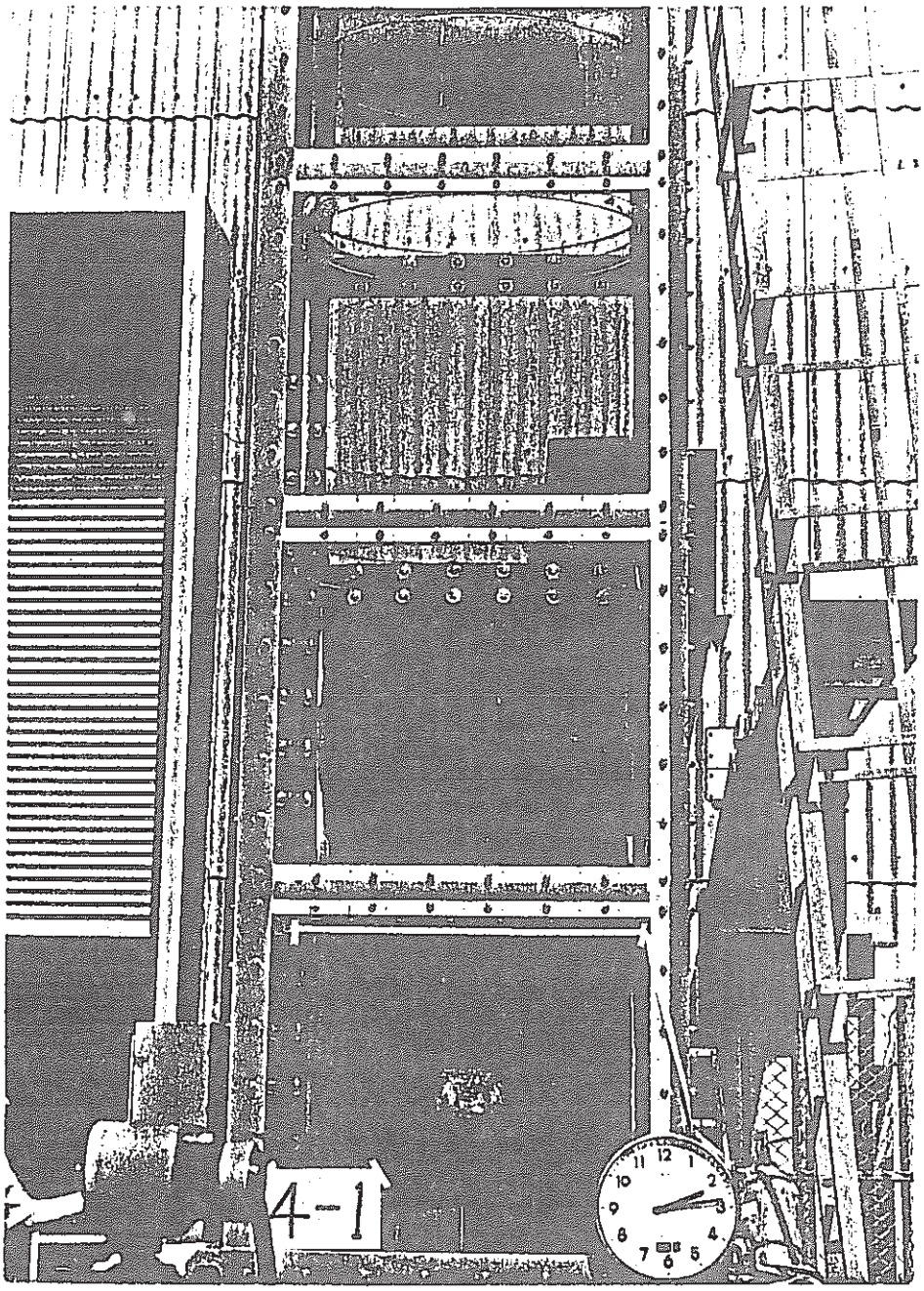

Fig. 25 Bubble Behavior Test Rig-I